

Luminescence



Efficient Luminescence from Fluorene- and Spirobifluorene-Based Lanthanide Complexes upon Near-Visible Irradiation

Gregorio Bottaro,^[a] Fabio Rizzo,^[b, c] Marco Cavazzini,^[b] Lidia Armelao,^{*,[a]} and Silvio Quici^{*,[b, c]}

Abstract: We describe herein the synthesis and photophysical characterization of new lanthanide complexes that consist of a (9,9-dimethylfluoren-2-yl)-2-oxoethyl or a (9,9'-spirobifluoren-2-yl)-2-oxoethyl unit as the antenna, covalently linked to a 1,4,7,10-tetraazacyclododecane-1,4,7-triacetic acid (DO3A) unit as the Ln³⁺ (Gd³⁺, Eu³⁺, Sm³⁺, Tb³⁺, Dy³⁺) coordination site. We were able to translate the spectroscopic properties of the innovative bipartite ligands into the forma-

tion of highly luminescent europium complexes that exhibit efficient emission ($\phi_{se} > 0.1$) upon sensitization in the near-visible region, that is, with an excitation wavelength above 350 nm. The luminescence of the Eu³⁺ complexes is clearly detectable at concentrations as low as 10 pM. Furthermore, the structural organization of these bipartite ligands makes the complexes highly soluble in aqueous solutions and chemically stable over time.

Introduction

The use of lanthanide complexes as luminescent probes in biochemical and biomedical applications represents a cutting-edge research field in which a steady increase in activity has been observed.^[1,2] Ideal candidates for practical applications in this field are represented by complexes that bear sensitizing antennae endowed with high solubility in water over a physiologically relevant pH range (typically 4–8) and excellent chemical stability over time and at sub-nanomolar concentrations.^[1–3]

The preparation of highly luminescent complexes that bear suitable coordination sites and sensitization units is a mandatory requisite to fully exploit the unique emission properties of lanthanide ions, that is, large Stokes shifts, narrow emission bands characteristics for each element of the rare-earth family, and long lifetimes (microsecond–millisecond range). Whereas enhanced measurement sensitivity can be easily obtained by exploiting the long-lived emission of the lanthanide elements for time-resolved homogeneous immunoassays,^[1,3,4] bright luminescence and excellent stability over a wide concentration range can be achieved only by properly designed complexes.

Over the past years, we have synthesized a variety of lanthanide complexes^[5–9] (mainly Eu³⁺ and Tb³⁺) with different cyclic and acyclic polydentate polyaminopolycarboxylates coordination sites, by following the so-called pendant chromophore strategy.^[1,7] This strategy implies the use of conceptually simple two-component ligands that consist of a single light-harvesting unit flexibly connected to a multidentate ligand through a methylene bridge.

Phenanthroline or acetophenone derivatives were used as efficient antenna systems owing to their high molar absorption coefficients (ϵ), high intersystem crossing efficiency, and favorable energy separation ($\approx 2000 \text{ cm}^{-1}$) between their excited triplet states and the Ln³⁺ emitting levels.^[10,11] The complexes showed high solubility and stability in aqueous medium, and high overall photoluminescence quantum yields (up to 0.45) in aqueous solution and in silica thin films upon UV-light excitation.

Although high efficiency has been attained, the possibility to shift the wavelength of excitation from medium UV towards the visible region by using chromophores that absorb light above 350 nm should result in beneficial practical implications.

In fact, especially in immunoassay applications, this should facilitate the use of easily available excitation sources and avoid the use of expensive quartz optics, limit the degradation of biomolecules, which is severe upon UV irradiation, and reduce spectral interference (below 320 nm) owing to the auto-fluorescence of tissues.^[12–14] In this regard, efficient europium and terbium emission at long excitation wavelength has been previously reported using *N*-alkyl acridones, azathiaxanones, and hydroxyisophthalamides as chromophores.^[4,15–18]

We are presenting in this study two series of innovative luminescent lanthanide antenna complexes in which the light-harvesting unit is bonded to the 1,4,7,10-tetraazacyclododecane-1,4,7-triacetic acid (DO3A),^[5,19] a macrocyclic multidentate ligand that acts as a highly effective hosting unit for the Ln³⁺

[a] Dr. G. Bottaro, Dr. L. Armelao
IENI-CNR and INSTM, Dipartimento di Scienze Chimiche
Università di Padova, Via Marzolo 1, 35131 Padova (Italy)
E-mail: lidia.armelao@unipd.it

[b] Dr. F. Rizzo, Dr. M. Cavazzini, Dr. S. Quici
ISTM-CNR, Via Golgi 19, 20133 Milano (Italy)
E-mail: silvio.quici@istm.cnr.it

[c] Dr. F. Rizzo, Dr. S. Quici
ISTM-CNR and Polo Scientifico Tecnologico
Via Fantoli 15/16, 20138 Milano (Italy)

Supporting information for this article is available on the WWW under <http://dx.doi.org/10.1002/chem.201305029>. It includes detailed synthetic procedures of all new compounds, ¹H and ¹³C NMR spectra of all new compounds, and spectroscopic characterization of ligands and complexes at different T and concentration.

cations. 9,9-Dimethylfluorene and 9,9'-spirobifluorene were selected as the chromophores and linked to the DO3A unit through a short and flexible spacer that contained a ketone group that allows the binding on lanthanide ions when complexes are formed (Figure 1).^[8,19]

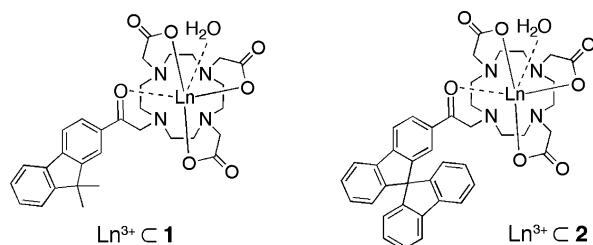


Figure 1. Structure of $\text{Ln}^{3+} \subset \mathbf{1}$ and $\text{Ln}^{3+} \subset \mathbf{2}$ complexes ($\text{Ln} = \text{Eu, Tb, Sm, Gd, Dy}$).

Fluorene and 9,9'-spirobifluorene derivatives with tailor-made optical and redox properties are being actively investigated as organic light-emitting materials for optoelectronics and in electro-generated chemiluminescence studies.^[20–22]

There is a great interest that surrounds spirobifluorene and fluorene since they can be chemically modified to tune the spectroscopic and electrochemical properties both in solution and in the solid state. By merging the unique properties of lanthanides and the versatility of fluorene and spirobifluorene molecules, a family of innovative complexes, supramolecular architectures, and functional materials can be developed. These aspects are particularly important to rationalize the chemical design and the preparation of highly efficient light-emitting systems and materials.

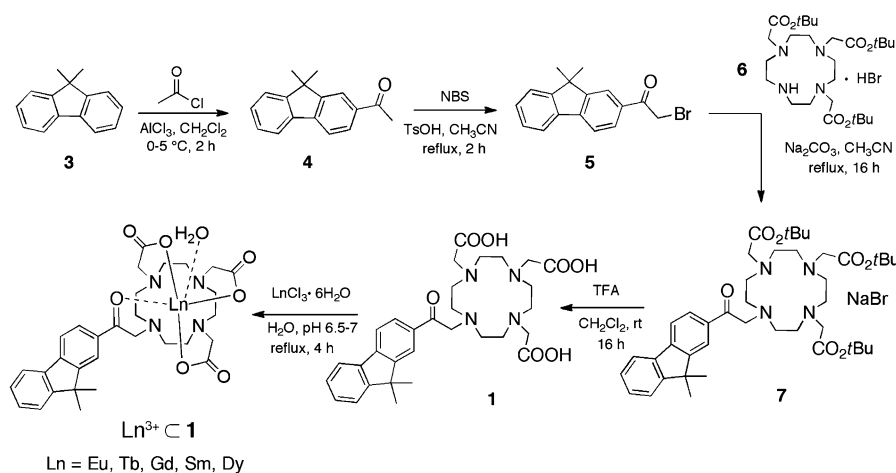
To the best of our knowledge, very few studies have appeared in the literature that report the use of fluorene and spirobifluorene derivatives as sensitizers for lanthanide emission. Moreover, the ligand-sensitizer system of the literature complexes is substantially different from the one described herein. In some cases, the coordination of the metal center is achieved by the assembly of different units^[23,24] around the Ln^{3+} rather than by a preorganized polydentate unit. Only in one case has a preformed and organized ligand been adopted, but the large distance between the antenna and the Eu^{3+} site, and the lack of short-range interaction between the donor and the acceptor result in low photoluminescence quantum yields (0.08 in CH_2Cl_2).^[25] None of these studies reports the use of water as solvent, and the luminescence data refer to the compounds in

the solid state or in solution of organic solvents (DMSO or CH_2Cl_2). At variance, the complexes here reported show 1) remarkable thermodynamic stability and kinetic inertness owing to the employment of a preorganized polydentate ligand, 2) an effective antenna-to-lanthanide energy transfer thanks to the favorable energy matching between the chromophore triplet states and lanthanide emitting levels, and, 3) most importantly, efficient luminescence at excitation wavelength higher than 350 nm and at concentrations as low as the picomolar level thanks to the peculiar spectroscopic properties of the sensitizers.

Results and Discussion

Synthesis of the ligands and complexes

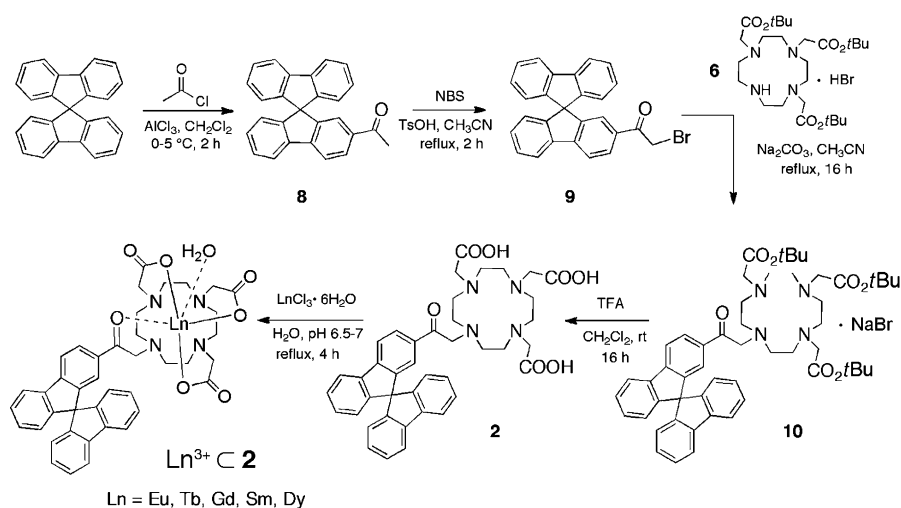
We synthesized bipartite ligands **1** and **2** (see Schemes 1 and 2) that feature a (9,9-dimethylfluorene-2-yl)-2-oxoethyl and a (9,9'-spirobifluorene-2-yl)-2-oxoethyl unit as the antenna, re-



Scheme 1. Synthesis of ligand **1** and the corresponding $\text{Ln}^{3+} \subset \mathbf{1}$ complexes.

spectively, which are covalently linked to a 1,4,7,10-tetraazacyclododecane-1,4,7-triacetic acid (DO3A) unit as the Ln^{3+} coordination site. The choice of these chromophores as antennae was mainly on account of their triplet energy levels, which promote sensitization of lanthanide luminescence in the range of wavelengths between 350 and 420 nm. Furthermore, similarly to acetophenone^[5] they coordinate the lanthanide cation through the carbonyl group, thus ensuring efficient energy-transfer processes from the antenna to the complexed metal. DO3A was selected as the Ln -chelating subunit because of its high thermodynamic and kinetic stabilities, which have been thoroughly assessed for its lanthanide complexes.^[26]

Ligand **1** and the corresponding complexes $\text{Ln}^{3+} \subset \mathbf{1}$ were synthesized according to Scheme 1. 9,9-Dimethylfluorene (**3**) and 2-acetyl-9,9-dimethylfluorene (**4**) were prepared according to literature procedures.^[27] Treatment of **4** with *N*-bromosuccinimide (NBS) and *p*-toluenesulfonic acid (TsOH) in CH_3CN under reflux conditions for 2 h produced 2-bromo-1-(9,9-dimethyl-



Scheme 2. Synthesis of ligand **2** and the corresponding Ln³⁺ **2** complexes.

fluorene-2-yl)ethanone (**5**)^[28] in 84% yield after purification by silica gel column chromatography.

Alkylation of DO3A tris(*tert*-butyl) ester hydrobromide **6**^[29,30] with **5** was carried out in CH₃CN under reflux conditions in the presence of Na₂CO₃ as base to afford sodium bromide complex **7** in quantitative yield after column chromatography. Indeed the complexing ability of alkylated DO3A triesters to coordinate sodium cation has been already assessed^[9,31] and the presence of the sodium bromide complex simplifies the chromatographic purification and allows higher yields of isolated product. Decomplexation of **7** takes place during deprotection of the *tert*-butyl groups, which was achieved by treatment of **7** with CF₃COOH at room temperature and afforded the tricarboxylic acid derivative **1** as white solid in 85% yield after purification through a short Amberlite XAD 1600T column eluting with pure H₂O and H₂O/CH₃CN (1:1 v/v). The Eu³⁺ **1** complex was prepared by the addition of a solution of EuCl₃·6H₂O in H₂O into a water solution of the ligand **1** under magnetic stirring and adjusting the pH at 6.5–7.0 with 2% aqueous NaOH. The reaction mixture was then heated at reflux for 4 h. Purification of the residue by a short Amberlite XAD 1600T column eluting first with pure H₂O to remove all inorganic salts and then with H₂O/CH₃CN (1:1 v/v) afforded the Eu³⁺ **1** in 89% yield as a white crystalline solid. All the lanthanide complexes—namely, Tb³⁺ **1**, Sm³⁺ **1**, Dy³⁺ **1**, and Gd³⁺ **1**—were prepared by following a procedure similar to that used for Eu³⁺ **1**. Ligand **2** and the corresponding complexes Ln³⁺ **2** were synthesized according to Scheme 2 by following synthetic procedures similar to those described above (Scheme 1) starting from 2-bromo-1-(9,9'-spirobifluorene-2-yl)ethanone (**9**). 2-Acetyl-9,9'-spirobifluorene (**8**) was prepared from the commercially available 9,9'-spirobifluorene by a modified literature procedure.^[32,33]

Absorption properties of bipartite ligands **1** and **2**

Fluorene, 9,9'-spirobifluorene, and their derivatives are widely employed as strong blue or green emitters for organic optoe-

lectronic applications. They can be chemically modified with a large variety of donor and/or acceptor groups to tune their electronic and optical properties. The high versatility of the chemistry of these molecules was recently exploited to synthesize molecules that bear fluorene and spirobifluorene cores that show nonlinear optical or high emissive properties and electrochemiluminescent behavior.^[20–22] Spirobifluorene is characterized by two fluorene units connected through the spiro carbon atom. This particular spatial configuration induces strong rigidity and increases the stability of the

system, thereby hampering the oxidation process that usually occurs at position 9 of the fluorene ring.^[20] For this reason, the fluorene derivative used as a sensitizer for lanthanide emission in this study has been substituted with two methyl groups in position 9.

Absorption of ligands **1** and **2** and of the corresponding Eu³⁺ **1** and Eu³⁺ **2** complexes in water is reported in Figure 2a. The spectra of both ligand **1** and Eu³⁺ **1** are dominated by a strong single band in the UV region, which shows a bathochromic shift of approximately 20 nm in the complex. A very different band profile is observed for ligand **2** and for the corresponding Eu³⁺ **2** derivative. In fact, we observe a redshift of approximately 25 nm in the onset of the absorption bands and a new absorption maximum peak at around 325 nm. Spirobifluorene is characterized by two fluorene units connected through the spiro carbon atom. The presence of the spiro bridge is expected to only marginally affect the molecular properties. In fact spiro conjugation is weak relative to π conjugation because of the 90° twisted orientation of the molecular fragments involved in the spiro bond, which minimizes mutual electrostatic interactions.^[22,34] Owing to this particular conjugation, the presence of Ln³⁺ ions represents a much stronger perturbation for the energy levels of the fluorene moiety to which the DO3A unit is bonded, thus affecting its absorption properties and leaving the other half of the molecule only slightly perturbed. To assign the absorption peaks, a solvatochromism experiment was performed in a series of solvents characterized by different dielectric constant and hydrogen-bonding characteristics (see the Kamlet–Taft parameters in Figure 2).

The absorption spectra of spirobifluorene, reported in Figure 2b, show two narrow peaks, the shape and position of which are very slightly affected by the nature of the solvent.

The same behavior is observed for fluorene (Figure S17 in the Supporting Information). From these results, we can attribute the narrow peaks of Ln³⁺ **2** complexes (Figure 2c) to transitions localized on the bare fluorene part. In addition, we observe (Figure 2c) a series of transitions related to the spirobi-

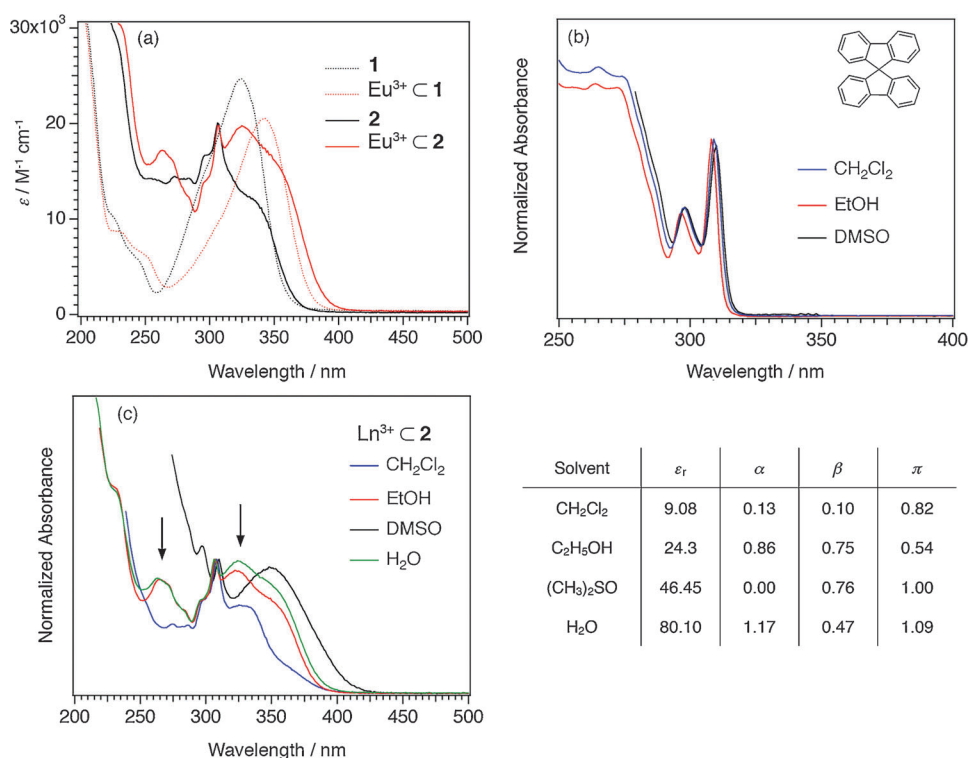


Figure 2. Absorption spectra of a) bipartite ligands **1** and **2**, and of the corresponding $\text{Eu}^{3+} \subset \mathbf{1}$ and $\text{Eu}^{3+} \subset \mathbf{2}$ complexes in aqueous solution (10^{-5} M); b) spirobifluorene in different solvents, and c) $\text{Ln}^{3+} \subset \mathbf{2}$ complexes in different solvents. The dielectric constant values and the Kamlet–Taft parameters^[35] are reported for the selected solvents.

fluorene part linked to the DO3A ligand, the profile of which is heavily influenced by the nature of the medium. The arrows in Figure 2c indicate a set of transitions that could be related to the carbonyl moiety of the $\text{Ln}^{3+} \subset \mathbf{2}$ complex since they are influenced by the solvent proticity and hydrogen-bonding capacity. However, the bands at high wavelengths show the typical behavior of $\pi \rightarrow \pi^*$ transitions that result in a redshift upon an increase in the solvent dielectric constant.^[36–39]

As previously highlighted, chromophores that absorb light above 350 nm are highly sought after and represent a challenge for the design of lanthanide complexes for biological and biomedical applications. From the spectra reported in Figure 2a, it is evident that the bipartite ligands **1** and **2** have transitions well beyond this threshold value. A further necessary requisite to this end is the favorable energy gap between the excited triplet states of the chromophores and the Ln^{3+} -emitting levels. The energies of the triplet states of ligands **1** and **2** involved in the energy-transfer events that promote the sensitized lanthanide emission^[10,11,40] have been experimentally evaluated by measuring the phosphorescence of the related Gd^{3+} complexes, as reported below.

Phosphorescence study of $\text{Gd}^{3+} \subset \mathbf{1}$ and $\text{Gd}^{3+} \subset \mathbf{2}$ complexes

At room temperature, the emission spectra of ligand **1** and $\text{Gd}^{3+} \subset \mathbf{1}$ (Figure S18b in the Supporting Information) excited at the corresponding absorption maximum (Figure S18a in the Supporting Information) are quite similar and are characterized

by the presence of a single broad band, which is only slightly different to the position of the maximum, in analogy to the behavior previously evidenced in the absorption spectra shown in Figure 2a. To get a deeper insight into the nature of the involved electronic transitions, the phosphorescence spectra of $\text{Gd}^{3+} \subset \mathbf{1}$ and $\text{Gd}^{3+} \subset \mathbf{2}$ were recorded at low temperature (77 K). The emission spectra (Figure 3a) present a more complex profile, with a number of bands and their relative intensities strongly dependent on the excitation wavelength.

From the spectra reported in Figure 3b, it clearly appears that in the $\text{Gd}^{3+} \subset \mathbf{1}$ complex there are two distinct triplet states, the energy values of which are $T_1(\mathbf{1}) = 22990 \text{ cm}^{-1}$ (435 nm) and $T_2(\mathbf{1}) = 20408 \text{ cm}^{-1}$ (490 nm). Upon excitation into the high-energy electronic transitions (280 nm), both $T_1(\mathbf{1})$ and $T_2(\mathbf{1})$ can be populated, whereas at

lower excitation energy (340 nm), emission only from the latter is observed. All the other bands present in Figure 3a have been assigned to singlet levels since their intensity vanishes if emission is recorded over a time window delayed by 50 μs after excitation. In Figure 3, we can also observe a vibronic progression with energy of 1450 cm^{-1} . To obtain a complete knowledge of the emission properties of $\text{Gd}^{3+} \subset \mathbf{1}$, we estimated the phosphorescence lifetimes of the two triplet levels. A difference higher than one order of magnitude was found between the τ value (680 ms) of the high-energy triplet state ($T_1(\mathbf{1})$: $\lambda_{\text{exc}} = 280 \text{ nm}$, $\lambda_{\text{em}} = 435 \text{ nm}$) and the one (15 ms) of the low-energy triplet state ($T_2(\mathbf{1})$: $\lambda_{\text{exc}} = 348 \text{ nm}$; $\lambda_{\text{em}} = 490 \text{ nm}$).

As a general rule, the absorption spectra are generated from n, π^* and π, π^* transitions, and the phosphorescence spectra are due to $^3(n, \pi^*)$ and/or $^3(\pi, \pi^*)$ triplet levels. In aryl ketones that bear strong donating groups, charge-transfer bands from the substituent to the carbonyl group are also possible.

Owing to the difference in the involved initial and final states (i.e., $^3(n, \pi^*)$ and/or $^3(\pi, \pi^*)$), the nature of the lowest-lying levels is strongly dependent on the solvent (e.g., polarity, hydrogen-bonding capability).^[41–45] Despite the different solvatochromic behavior, the two kinds of triplet levels can be discriminated through their phosphorescence lifetimes being, at 77 K, in the millisecond range for $^3(n, \pi^*)$ and 10–1000 times longer for $^3(\pi, \pi^*)$.^[44] On this basis, the low-energy triplet of $\text{Gd}^{3+} \subset \mathbf{1}$ is attributed to the n, π^* type that involves the carbonyl group directly bonded to the metal ion. Therefore, if this level is energetically suitable to sensitize lanthanide emission,

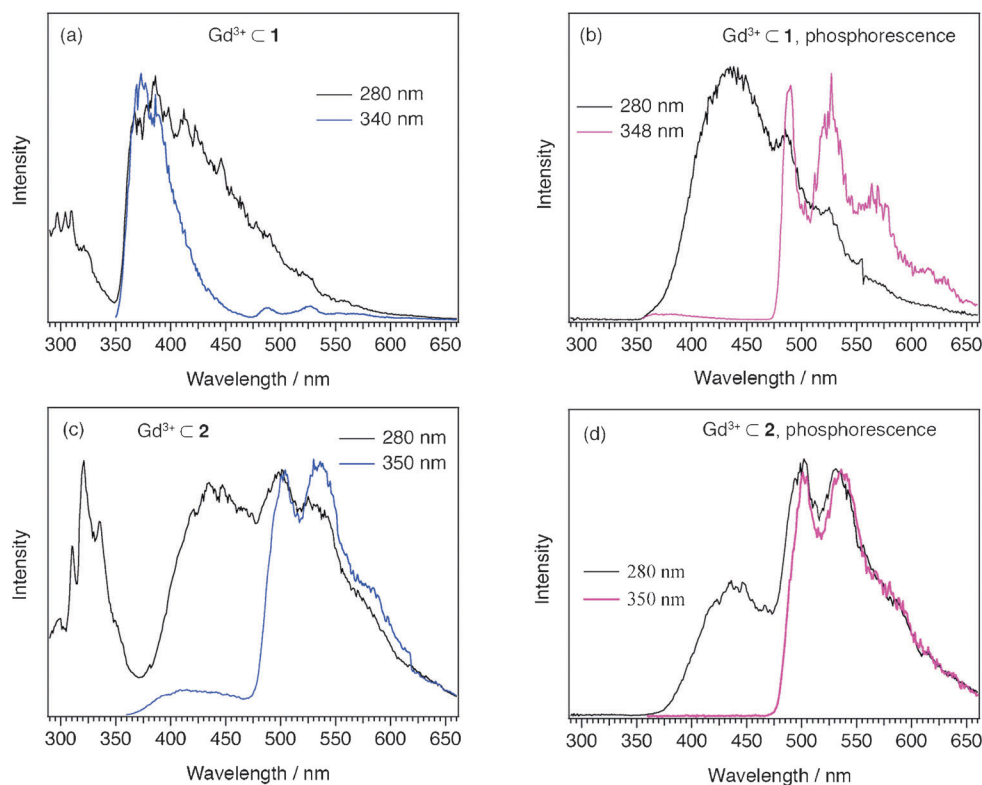


Figure 3. Emission spectra at 77 K excited at different wavelengths for 10^{-5} M solutions of a) $\text{Gd}^{3+} \subset \mathbf{1}$ fluorescence (steady state), b) phosphorescence spectra (50 μs delay after pulse), c) $\text{Gd}^{3+} \subset \mathbf{2}$ fluorescence (steady state), and d) phosphorescence spectra (50 μs delay after pulse). For all solutions, a methanol/ethanol mixture (1:1 v/v) has been used as the solvent. The energy values of the triplet levels for spirobifluorene and fluorene derivatives are listed in Table 1.

the excitation wavelength can be pushed well beyond 350 nm as demonstrated by the complex excitation spectra (Figure S19 in the Supporting Information).

By taking into account the energy match condition for the involved levels, the $T_2(1)$ triplet ($20\,408\text{ cm}^{-1}$) should be able to sensitize the emission of Eu^{3+} (${}^5\text{D}_0$, $17\,250\text{ cm}^{-1}$) and Sm^{3+} (${}^4\text{G}_{5/2}$, $17\,800\text{ cm}^{-1}$), the emitting states of which lie more than 2000 cm^{-1} lower in energy, but not the emission of Tb^{3+} (${}^5\text{D}_4$, $20\,430\text{ cm}^{-1}$) and Dy^{3+} (${}^4\text{F}_{9/2}$, $20\,960\text{ cm}^{-1}$).^[11,40] At variance, it is worth noting that the energy of $T_1(1)$ ($22\,990\text{ cm}^{-1}$) is suitable for the sensitization of all lanthanide ions emitting in the visible region. The behavior of $\text{Gd}^{3+} \subset \mathbf{2}$ is very close to the one observed for $\text{Gd}^{3+} \subset \mathbf{1}$; the spectral features have been found to be dependent on the excitation wavelength, and the phosphorescence spectra (50 μs delay time) revealed the presence of two distinct triplet levels with energy $T_1(2) = 22\,727\text{ cm}^{-1}$ (440 nm) and $T_2(2) = 20\,000\text{ cm}^{-1}$ (500 nm). The corresponding lifetimes are comparable to those determined for $\text{Gd}^{3+} \subset \mathbf{1}$, their value being $\tau(T_1(2)) = 638\text{ ms}$ ($\lambda_{\text{exc}} = 280\text{ nm}$; $\lambda_{\text{em}} = 440\text{ nm}$) and $\tau(T_2(2)) = 12\text{ ms}$ ($\lambda_{\text{exc}} = 350\text{ nm}$; $\lambda_{\text{em}} = 500\text{ nm}$). Accordingly, the triplet transitions have been assigned as for the $\text{Gd}^{3+} \subset \mathbf{1}$ complex. As it can be observed, the energy of the $\text{Gd}^{3+} \subset \mathbf{2}$ triplet levels is slightly lower than the corresponding transitions for $\text{Gd}^{3+} \subset \mathbf{1}$. Moreover, the absorption and excitation spectra (see Figure S20 in the Supporting Information) of the spirobifluorene derivative are more extended toward the

visible region, thereby disclosing the possibility of sensitizing lanthanide emission upon excitation at longer wavelengths. Finally, the presence of the spiro-bridge does not seem to have any influence on the spectroscopic properties of both ligand **2** and the corresponding $\text{Gd}^{3+} \subset \mathbf{2}$ complex.

Spectroscopy of $\text{Eu}^{3+} \subset \mathbf{1}$ and $\text{Eu}^{3+} \subset \mathbf{2}$ complexes

The excitation and emission spectra of $\text{Eu}^{3+} \subset \mathbf{1}$ are reported in Figure 4. Interestingly, the excitation and absorption spectra are completely overlapped; this allows sensitization of europium luminescence over a large spectral range. In $\text{Eu}^{3+} \subset \mathbf{1}$, fluorene can act as antenna through both of its triplet levels (see Figure 3), but the higher emission intensity is reached by exploiting the lower energy one ($T_2(1)$), the excitation maximum of which is at approximately 350 nm (Figure S19 in the Supporting Information). Quite remarkably, europium emission can be achieved upon excitation well over 350 nm, up to the boundary with the visible region (Figure 4c).

Between 550 and 750 nm the spectrum is dominated by emission from the Eu^{3+} centers, which is composed of several bands associated with ${}^5\text{D}_0 \rightarrow {}^7\text{F}_J$ transitions ($J = 0, 1, 2, 3, \text{ and } 4$); the higher the J value, the lower the transition energy (Figure 4b).^[46] We observed an abnormal intensity of the ${}^5\text{D}_0 \rightarrow {}^7\text{F}_4$ transition that has been reported in literature only in a few cases.^[47,48] Ferreira et al. have theoretically interpreted this behavior in terms of the Ω_λ intensity parameters and their dependence on the nature and local symmetry of the chemical environment around the Eu^{3+} ion, thus leading to the conclusion that the chemical environment is highly polarizable with a local symmetry that corresponds to a slightly distorted D_{4d} coordination geometry.^[47] We can hypothesize a similar explanation in our case as well, although the structure of the complexes has not been yet determined owing to the difficulty in obtaining good crystals.

The sensitized lanthanide emission is clearly perceived upon tuning the excitation wavelength up to 400 nm, at which point the UV region fades into the visible band (Figure 4c, inset). Despite the expected overall reduced intensity owing to the lower absorbance value of the antenna, the spectrum displays all europium components with comparable resolution to that observed upon excitation at 345 nm, that is, into the maximum of the excitation band. As previously emphasized, the optimal

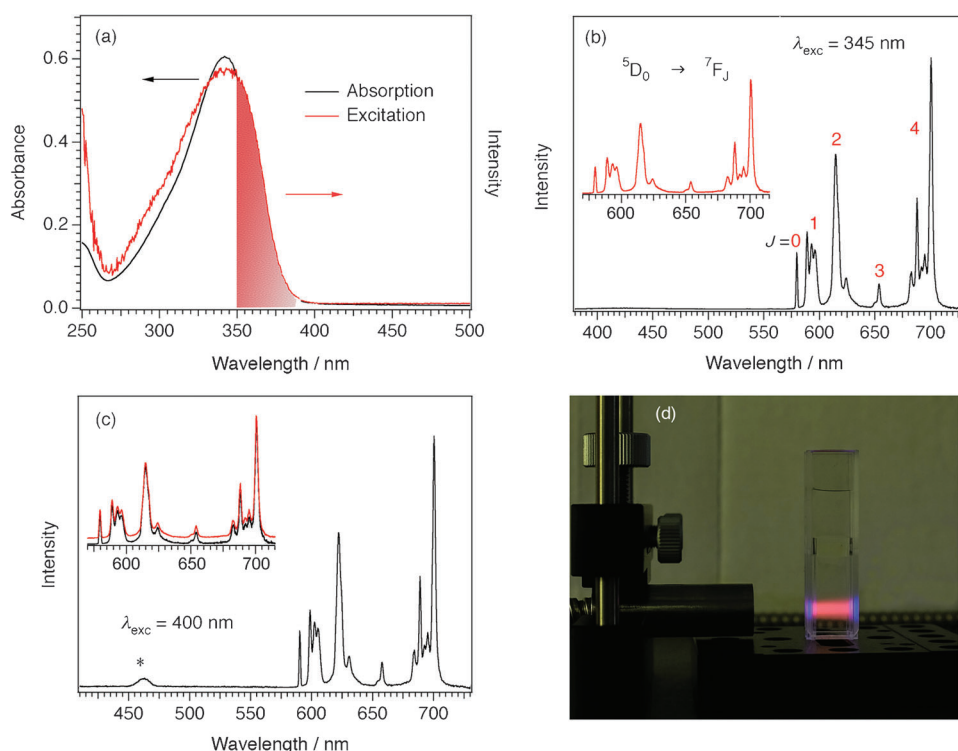


Figure 4. a) Absorption and excitation spectra monitored at $\lambda_{em}=615$ nm, and b) emission spectrum of $\text{Eu}^{3+}\text{C} 1$ (10^{-5} M water solution) excited at 345 nm. The details of the spectrum are reported in the inset. c) Emission spectrum of $\text{Eu}^{3+}\text{C} 1$ (10^{-5} M water solution) excited at 400 nm. The water Raman band is highlighted with an asterisk in the spectrum. In the inset are reported the high-resolution spectra at two different excitation wavelengths: 345 (red curve) and 400 nm (black curve). d) Emission from a $\text{Eu}^{3+}\text{C} 1$ water solution (10^{-5} M) in a polymethylmethacrylate (PMMA) cuvette illuminated at 380 nm with a Xe lamp.

spectroscopic compatibility of such complexes with low-cost polymeric optical materials represents a substantial advantage for practical applications. As highlighted in Figure 4d, a bright red emission is clearly visible with the naked eye from $\text{Eu}^{3+}\text{C} 1$ aqueous solutions (10^{-5} M) in a polymethylmethacrylate (PMMA) cuvette excited at $\lambda=380$ nm. A further major qualification for fluorescent probes to be used in biochemical and biomedical applications concerns their chemical stability in the very low concentration range. The luminescence performances of $\text{Eu}^{3+}\text{C} 1$ fulfill this requirement as its emission is still detectable at concentrations as low as 10 pM (Figure S21 in the Supporting Information). Although the presence of free Eu^{3+} ions cannot be completely ruled out, the observed emissions are unambiguously attributed to the $\text{Eu}^{3+}\text{C} 1$ complex. Indeed, this is the only species capable of emitting light at 615 nm upon excitation at 345 nm. For the spirobifluorene derivative $\text{Eu}^{3+}\text{C} 2$, the whole absorption band (Figure 5a) can be exploited for the sensitization of europium emission thanks to the suitability of all transitions to populate the low-energy triplet level $T_2(2)$ at 20000 cm^{-1} .

The number of J multiplets, their position, and their relative intensity are very similar in the $\text{Eu}^{3+}\text{C} 1$ and $\text{Eu}^{3+}\text{C} 2$ complexes, clearly indicating an equivalent local coordination geometry for the Eu^{3+} sites^[10,11,49] despite the presence of a bulkier chromophore in $\text{Eu}^{3+}\text{C} 2$. It is worth highlighting that in $\text{Eu}^{3+}\text{C} 2$ the presence of the spirobifluorene unit allows the

sensitized emission to occur up to excitation wavelengths of 420 nm, that is, 20 nm longer relative to $\text{Eu}^{3+}\text{C} 1$ (Figure 5b,c). Similarly to $\text{Eu}^{3+}\text{C} 1$, $\text{Eu}^{3+}\text{C} 2$ shows chemical stability in highly diluted aqueous solutions (≈ 10 pM); emission spectra of $\text{Eu}^{3+}\text{C} 2$ at decreasing concentrations are shown in Figure S22 of the Supporting Information.

By surveying the light response from diluted aqueous solutions (1 nM) of both europium complexes over time, we noticed a steady behavior upon aging under ambient conditions. The emission spectra measured at regular intervals up to several months (Figure S23 in the Supporting Information) indicate a very high stability even at subnanomolar concentrations and an excellent reproducibility of color chromaticity.

The photophysical data for $\text{Eu}^{3+}\text{C} 1$ and $\text{Eu}^{3+}\text{C} 2$ complexes are summarized in Table 1. Both $\text{Eu}^{3+}\text{C} 1$ and $\text{Eu}^{3+}\text{C} 2$ show absolute quantum

Table 1. Photophysical data of europium complexes.		
	$\text{Eu}^{3+}\text{C} 1$	$\text{Eu}^{3+}\text{C} 2$
λ_{max} [nm]	345	345 (325)
ϵ [$\text{M}^{-1}\text{ cm}^{-1}$]	20312	17152 (19792)
T_1 [cm^{-1}]	22990	22727
T_2 [cm^{-1}]	20408	20000
$\tau_{\text{H}_2\text{O}}$ [ms]	0.605	0.598
$\tau_{\text{D}_2\text{O}}$ [ms]	2.097	2.134
ϕ_{se} in H_2O	0.12 ^[a] (0.12) ^[b]	0.14 ^[a] (0.12) ^[b]
ϕ_{se} in D_2O	0.36 ^[a]	0.38 ^[a]
q ^[c]	1 \pm 0.5	1 \pm 0.5

[a] Quantum yield values obtained by using the integrating sphere ($\lambda_{exc}=345$ nm). [b] Quantum yield values obtained by using $[\text{Ru}(\text{bpy})_3]\text{Cl}_2$ as standard ($\lambda_{exc}=345$ nm). [c] Number of water molecules in the first coordination shell estimated by the Horrocks formula: $q_{Eu}=1.11(1/\tau_{\text{H}_2\text{O}}-1/\tau_{\text{D}_2\text{O}}-0.31)$.

yields higher than 10%, and the excited-state dynamics for the $^5\text{D}_0 \rightarrow ^7\text{F}_2$ transition are characterized by a single exponential decay (Figure S24 in the Supporting Information).

The remarkable increase of the photoluminescence yields and the decay lifetimes determined in D_2O for both complexes indicate the presence of water in the first coordination sphere of the metal. On the basis of the Horrocks equation,^[50–53] we estimated the presence of one coordinated solvent molecule at each europium center (Table 1).

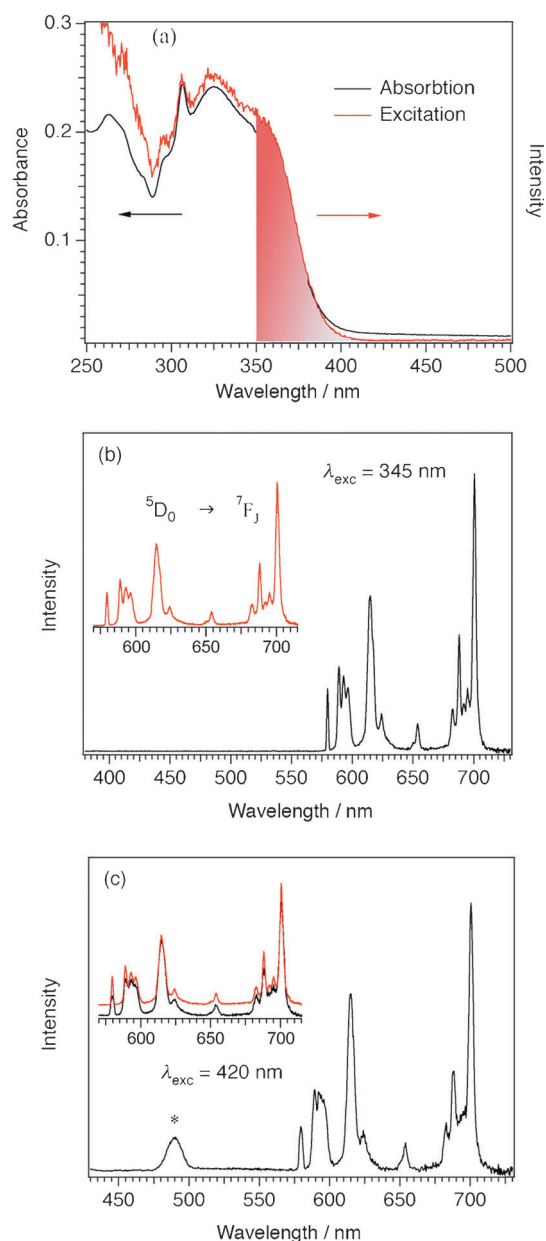


Figure 5. a) Absorption and excitation spectra monitored at $\lambda_{em} = 615$ nm, and b) emission spectra excited at 345 nm of 10^{-5} M $\text{Eu}^{3+} \subset \mathbf{2}$ aqueous solution. Details of the europium emission spectrum are reported in the inset of (b). c) Emission spectra of $\text{Eu}^{3+} \subset \mathbf{2}$ in water (10^{-5} M solution) excited at 420 nm. The Raman band of water is highlighted with an asterisk in the spectrum. In the inset are reported the high-resolution spectra at two different excitation wavelengths: 345 (red curve) and 420 nm (black curve).

Emissive lanthanide complexes for use as tags in bioassays or as optical probes require both a high emission quantum yield and large molar absorptivity at an excitation wavelength above 330 nm to give high brightness, B , in which $B = \epsilon\phi$.^[54] In aqueous media, no europium complexes have been reported with a brightness ($\lambda_{exc} = 337$ nm) that exceeds $3000 \text{ M}^{-1} \text{ cm}^{-1}$. Our systems work quite well for europium emission. For excitation at 345 nm, the brightness is $2440 \text{ M}^{-1} \text{ cm}^{-1}$ for $\text{Eu}^{3+} \subset \mathbf{1}$ and $2400 \text{ M}^{-1} \text{ cm}^{-1}$ for $\text{Eu}^{3+} \subset \mathbf{2}$. Values of around 25000 – $30000 \text{ M}^{-1} \text{ cm}^{-1}$ are reported for the best systems.^[13]

Since the stability of the luminescent systems under continuous irradiation is a key factor for most applications such as sensing, bio-probing, lighting, and so on, and a high resistance towards photoinduced damages is required to improve the service life of molecules, we evaluated the photostability of the solid $\text{Eu}^{3+} \subset \mathbf{1}$ and $\text{Eu}^{3+} \subset \mathbf{2}$ complexes under continuous irradiation at $\lambda = 345$ nm. The integrated intensity was monitored as a function of the exposure time (Figure 6). The emission intensity decreases to approximately 50% of the initial value after 8 h irradiation, thereby evidencing a moderate stability toward photobleaching of the chromophore.

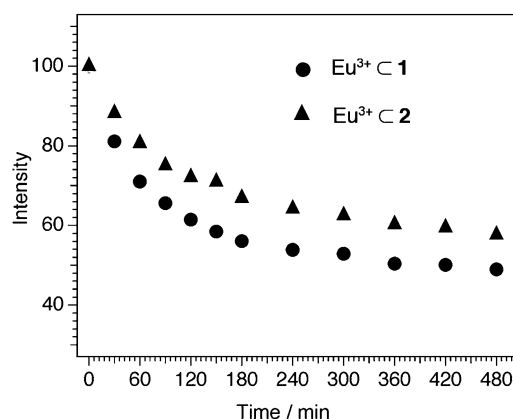


Figure 6. Photodecomposition profiles ($\lambda_{exc} = 345$ nm) for the solid $\text{Eu}^{3+} \subset \mathbf{1}$ and $\text{Eu}^{3+} \subset \mathbf{2}$ complexes.

The photodegradation process has been observed in a variety of lanthanide complexes including β -diketonate chelates, carboxylates and their derivatives, cryptates, and others. Their degradation under UV irradiation involves a series of complicated processes, often attributed to photobleaching or photon-induced chemical damage, although it has not been yet completely elucidated. Very recently an unprecedented improved photostability for Eu^{3+} and Gd^{3+} β -diketonate complexes has been reported for the first time, which is related to a *trans-to-cis* photoisomerization process of the photoactive ligand.^[46] A direct comparison of the photostability of different complexes is difficult since a great variability in experimental conditions has been reported in the literature. Photostability is measured over time ranges from a few minutes up to tens of hours on the pristine complexes or on the compounds dissolved in solution or dispersed in solid matrices. Cases that are very comparable with our results report emission losses that range from 30 to 50% over a time range from 80 min to 10 h.^[55–57]

Spectroscopy of $\text{Ln}^{3+} \subset \mathbf{1}$ and $\text{Ln}^{3+} \subset \mathbf{2}$ complexes (Ln = Sm, Dy, Tb)

Along with europium, three further lanthanide elements considered to be of great interest for their emission in the visible region are samarium, dysprosium, and terbium. Therefore, bipartite ligands **1** and **2** were used to prepare the correspond-

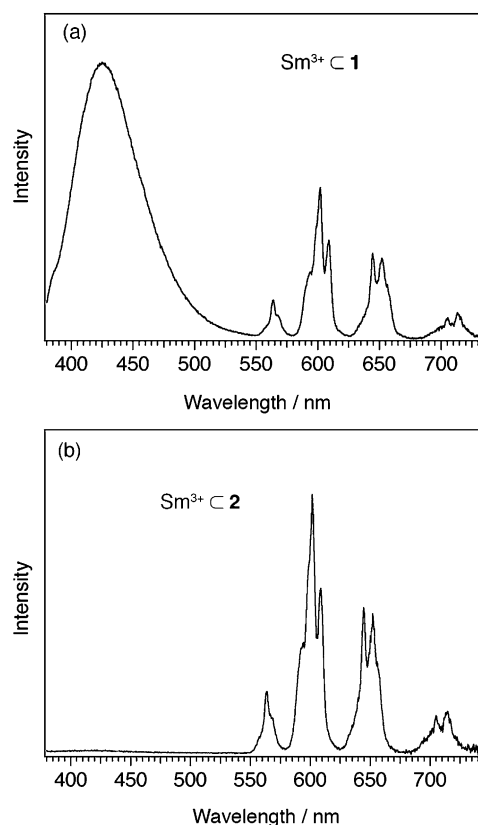


Figure 7. Emission spectra of a) $\text{Sm}^{3+} \subset \mathbf{1}$ ($\lambda_{\text{exc}} = 345 \text{ nm}$) and b) $\text{Sm}^{3+} \subset \mathbf{2}$ ($\lambda_{\text{exc}} = 325 \text{ nm}$) in aqueous solutions (10^{-5} M).

ing $\text{Ln}^{3+} \subset \mathbf{1}$ and $\text{Ln}^{3+} \subset \mathbf{2}$ complexes. In the case of $\text{Sm}^{3+} \subset \mathbf{1}$ and $\text{Sm}^{3+} \subset \mathbf{2}$, the sensitized emission from water solutions (10^{-5} M) is clearly detected, as shown in Figure 7.

The spectrum of both complexes is characterized by four main emission bands around 560, 600, 650, and 710 nm, which are assigned to the intraconfigurational 4f transitions from the $^4\text{G}_{5/2}$ excited state level to the $^6\text{H}_{5/2}$, $^6\text{H}_{7/2}$, $^6\text{H}_{9/2}$, and $^6\text{H}_{11/2}$ ground levels, respectively.^[58] In the spectrum of $\text{Sm}^{3+} \subset \mathbf{1}$ (Figure 7a) we also observe a relevant luminescence contribution between 400 and 500 nm owing to ligand-centered emission. This contribution is instead completely absent in $\text{Sm}^{3+} \subset \mathbf{2}$ (Figure 7b). The absolute quantum yields evaluated for the metal-centered emission are comparable for the two complexes (Table 2). Despite the low absolute values, these data are remarkable for samarium complexes in aqueous solutions.^[7] Higher quantum yields (0.007) have been recently reported for samarium derivatives excited at 274 nm.^[59]

Table 2. Room-temperature luminescence data in water solution.		
	$\text{Sm}^{3+} \subset \mathbf{1}$	$\text{Sm}^{3+} \subset \mathbf{2}$
λ_{max} [nm]	345	325
ϕ_{se}	0.0014, ^[a] 0.0020 ^[b]	0.0012, ^[a] 0.0017 ^[b]

[a] Quantum yield values obtained by using the integrating sphere ($\lambda_{\text{exc}} = 345 \text{ nm}$). [b] Quantum yield values obtained by using $[\text{Ru}(\text{bpy})_3]\text{Cl}_2$ as standard ($\lambda_{\text{exc}} = 345 \text{ nm}$).

In $\text{Tb}^{3+} \subset \mathbf{1}$ and $\text{Tb}^{3+} \subset \mathbf{2}$ complexes, the emission can be sensitized through the high-energy triplet states of ligands $\mathbf{1}$ ($T_1(\mathbf{1})$) and $\mathbf{2}$ ($T_1(\mathbf{2})$) upon excitation into the high-energy portion of the corresponding absorption bands (Figure 2a). However, besides the typical terbium green emission, a relevant ligand-centered contribution to the total luminescence is observed in the visible region (Figure S25 in the Supporting Information). This contribution becomes predominant in $\text{Dy}^{3+} \subset \mathbf{1}$ and $\text{Dy}^{3+} \subset \mathbf{2}$, and metal-centered emissions are not observed. These findings point out the scarce sensitization efficiency of ligands $\mathbf{1}$ and $\mathbf{2}$ toward Tb^{III} and Dy^{III} emission. The emission ineffectiveness due to back-energy transfer has been checked by measuring the spectra of all complexes after deaeration. We observed that, whereas the $\text{Dy}^{3+} \subset \mathbf{1}$ and $\text{Dy}^{3+} \subset \mathbf{2}$ spectra do not present any variation, a sensitive decrease of the ligand-centered emission is found only for $\text{Tb}^{3+} \subset \mathbf{2}$ (Figure S26 in the Supporting Information).

Conclusion

We have reported the synthesis and photophysical behavior of lanthanide complexes that feature fluorene and spirobifluorene chromophores as efficient light-harvesting units in the near-visible region covalently linked to a preorganized polydentate macrocycle as a highly effective ligand for the Ln^{III} cations. The spectroscopic properties of both fluorene and 9,9'-spirobifluorene antennae, that is, the absorption behavior and the energy position of the triplet states, have been carefully determined and properly translated into an efficient sensitized europium emission upon excitation of the complexes well above the threshold value of 350 nm. The luminescence of $\text{Eu}^{3+} \subset \mathbf{1}$ and $\text{Eu}^{3+} \subset \mathbf{2}$ molecules is clearly detectable at concentrations as low as 10 μM . By exploiting the high versatility of the chemistry of fluorene and 9,9'-spirobifluorene molecules, their electronic and optical properties can be tuned with a large variety of donor and/or acceptor groups. We also report that the structural organization of the bipartite ligands renders the complexes of Eu^{III} , Sm^{III} , Dy^{III} , and Tb^{III} highly soluble in aqueous solutions and chemically stable over time. The information gained in this study is currently being applied to the development of new lanthanide molecular probes with higher-emission quantum yields that have the potential to provide new multifunctional molecules for biochemical and biomedical purposes.

Experimental Section

Materials and methods

All available chemicals and solvents were purchased from commercial sources and were used without any further purification. Thin-layer chromatography (TLC) was conducted on plates precoated with silica gel Si 60-F254 (Merck, Darmstadt, Germany). Column chromatography was conducted by using silica gel Si 60, 230–400 mesh, 0.040–0.063 mm (Merck, Darmstadt, Germany). ^1H and ^{13}C NMR spectra were recorded using a Bruker Avance 400 (400 and 100.6 MHz, respectively). Unless otherwise specified, all experiments were made at room temperature. Chemical shifts were re-

ported in parts per million downfield from SiMe₄ by using the residual proton (CHCl₃, δ = 7.26 ppm; CHD₂OD, δ = 3.30 ppm; (CHD₂)₂NCOD, δ = 2.75, 2.92 ppm; and (CD₃)₂NCOH, δ = 8.03 ppm) and carbon (CDCl₃, δ = 77.0 ppm; CD₃OD, δ = 49.1 ppm; (CD₃)₂NCOD, δ = 29.8, 34.9, and 163.1 ppm) solvent resonances as internal reference. Protons and carbon atoms assignments are based on homonuclear (¹H,¹H double quantum filtered COSY) and heteronuclear (¹H,¹³C HSQC, ¹H,¹³C HMBC) correlation experiments. High-resolution mass spectrum of complexes were obtained using an electrospray ion-trap mass spectrometer ICR-FTMS APEX II (Bruker Daltonics) by the Centro Interdipartimentale Grandi Apparecchiature (C.I.G.A.) University of Milano.

Spectroscopic characterization

Absorption spectra in the UV/Vis were performed on aqueous solutions using a double-beam CARYSE spectrophotometer with a spectral bandwidth of 1 nm. The luminescence spectra were recorded on water (or D₂O) solutions at room temperature using a Fluorolog-3 (Horiba Jobin-Yvon) spectrofluorimeter equipped with a double-grating monochromator in both the excitation and emission sides coupled to a R928P Hamamatsu photomultiplier and a 450 W Xe arc lamp as the excitation source. The emission spectra were corrected for detection and optical spectral response of the spectrofluorimeter through a calibration curve supplied by the manufacturer. The excitation spectra were corrected for the spectral distribution of the lamp intensity using a photodiode reference detector. Phosphorescence spectra were acquired using the same instrument by employing a pulsed Xe lamp as source and a liquid-nitrogen-filled Dewar for the measurements at 77 K. The luminescence lifetimes on the microsecond–millisecond scales were measured using a pulsed xenon lamp with variable repetition rate and elaborated with standard software fitting procedures. Absolute photoluminescence quantum yields were calculated by corrected emission spectra obtained from an apparatus that consisted of a Spectralon-coated integrating sphere accessory (4", F-3018, Horiba Jobin-Yvon) fitted in the fluorimeter sample chamber. Quantum yield determination was also performed using air-equilibrated [Ru(bpy)₃]Cl₂ (bpy = 2,2'-bipyridyl) water solutions as standard.^[60] Three independent measurements were carried out on each complex with an estimated error of $\pm 20\%$. Quantum yield values are independent of the excitation wavelength in the investigated range.

Room-temperature measurements were performed on aqueous solutions both air-equilibrated and deaerated under Ar for 1 h. A methanol/ethanol (1:1 v/v) solution was used as the solvent for both fluorene and spirobifluorene ligands and for the corresponding gadolinium complexes, and it was used for the low-temperature (77 K) measurements. Photostability tests were performed in the fluorimeter sample chamber by employing the 450 W Xe arc lamp. The solid samples were kept under continuous irradiation for up to 8 h with a constant power of 1 mW cm⁻² at 345 nm.

Acknowledgements

We thank Prof. Danilo Pedron (University of Padova), Dr. ssa Federica Mian (ISTM-CNR), and Dr. ssa Roberta Seraglia (IENI-CNR Padova) for helpful discussion. The MIUR is gratefully acknowledged for financial support through the FIRB (Rinome RBAP114AMK, ItaNanoNet RBPR05JH2P) and PRIN (Record 20097X4457) projects.

Keywords: antennas · fluorenes · lanthanides · luminescence · photophysics

- [1] E. G. Moore, A. P. S. Samuel, K. N. Raymond, *Acc. Chem. Res.* **2009**, *42*, 542–552.
- [2] J.-C. G. Bünzli, *Chem. Rev.* **2010**, *110*, 2729–2755.
- [3] J. D. Moore, R. L. Lord, G. A. S. Cisneros, M. J. Allen, *J. Am. Chem. Soc.* **2012**, *134*, 17372–17375.
- [4] J. Xu, T. M. Corneille, E. G. Moore, G.-L. Law, N. G. Butlin, K. N. Raymond, *J. Am. Chem. Soc.* **2011**, *133*, 19900–19910.
- [5] L. Armelao, G. Bottaro, S. Quici, M. Cavazzini, M. C. Raffo, F. Barigelletti, G. Accorsi, *Chem. Commun.* **2007**, 2911–2913.
- [6] L. Armelao, S. Quici, F. Barigelletti, G. Accorsi, G. Bottaro, M. Cavazzini, E. Tondello, *Coord. Chem. Rev.* **2010**, *254*, 487–505.
- [7] S. Quici, M. Cavazzini, G. Marzanni, G. Accorsi, N. Armaroli, B. Ventura, F. Barigelletti, *Inorg. Chem.* **2005**, *44*, 529–537.
- [8] S. Quici, M. Cavazzini, M. C. Raffo, L. Armelao, G. Bottaro, G. Accorsi, C. Sabatini, F. Barigelletti, *J. Mater. Chem.* **2006**, *16*, 741–747.
- [9] S. Quici, G. Marzanni, M. Cavazzini, P. L. Anelli, M. Botta, E. Gianolio, G. Accorsi, N. Armaroli, F. Barigelletti, *Inorg. Chem.* **2002**, *41*, 2777–2784.
- [10] G. F. de Sá, O. L. Malta, C. de Mello Donegá, A. M. Simas, R. L. Longo, P. A. Santa-Cruz, E. F. da Silva, Jr., *Coord. Chem. Rev.* **2000**, *196*, 165–195.
- [11] L. D. Carlos, R. A. S. Ferreira, V. de Zea Bermudez, S. J. L. Ribeiro, *Adv. Mater.* **2009**, *21*, 509–534.
- [12] N. Maindron, S. Poupard, M. Hamon, J.-B. Langlois, N. Ple, L. Jean, A. Romieu, P.-Y. Renard, *Org. Biomol. Chem.* **2011**, *9*, 2357–2370.
- [13] J. W. Walton, A. Bourdolle, S. J. Butler, M. Soulie, M. Delbianco, B. K. McMahon, R. Pal, H. Puschmann, J. M. Zwiher, L. Lamarque, O. Maury, C. Andraud, D. Parker, *Chem. Commun.* **2013**, *49*, 1600–1602.
- [14] C. P. Montgomery, B. S. Murray, E. J. New, R. Pal, D. Parker, *Acc. Chem. Res.* **2009**, *42*, 925–937.
- [15] C. P. Montgomery, D. Parker, L. Lamarque, *Chem. Commun.* **2007**, 3841–3843.
- [16] A. Dadabhoy, S. Faulkner, P. G. Sammes, *J. Chem. Soc. Perkin Trans. 2* **2002**, 348–357.
- [17] P. Atkinson, K. S. Findlay, F. Kielar, R. Pal, D. Parker, R. A. Poole, H. Puschmann, S. L. Richardson, P. A. Stenson, A. L. Thompson, J. Yu, *Org. Biomol. Chem.* **2006**, *4*, 1707–1722.
- [18] S. Petoud, S. M. Cohen, J.-C. G. Bünzli, K. N. Raymond, *J. Am. Chem. Soc.* **2003**, *125*, 13324–13325.
- [19] A. Beeby, L. M. Bushby, D. Maffeo, J. A. Gareth Williams, *J. Chem. Soc. Dalton Trans.* **2002**, 48–54.
- [20] F. Polo, F. Rizzo, M. Veiga-Gutierrez, L. De Cola, S. Quici, *J. Am. Chem. Soc.* **2012**, *134*, 15402–15409.
- [21] F. Rizzo, M. Cavazzini, S. Righetto, F. De Angelis, S. Fantacci, S. Quici, *Eur. J. Org. Chem.* **2010**, 4004–4016.
- [22] T. P. I. Saragi, T. Spehr, A. Siebert, T. Fuhrmann-Lieker, J. Salbeck, *Chem. Rev.* **2007**, *107*, 1011–1065.
- [23] S. Wang, J. Zhang, Y. Hou, C. Du, Y. Wu, *J. Mater. Chem.* **2011**, *21*, 7559–7561.
- [24] D. B. Ambili Raj, S. Biju, M. L. P. Reddy, *Dalton Trans.* **2009**, 7519–7528.
- [25] D. S. Oxley, R. W. Walters, J. E. Copenhafer, T. Y. Meyer, S. Petoud, H. M. Edenborn, *Inorg. Chem.* **2009**, *48*, 6332–6334.
- [26] D. E. Reichert, J. S. Lewis, C. J. Anderson, *Coord. Chem. Rev.* **1999**, *184*, 3–66.
- [27] N. Lardiés, I. Romeo, E. Cerrada, M. Laguna, P. J. Skabara, *Dalton Trans.* **2007**, 5329–5338.
- [28] J. C. Lee, Y. H. Bae, S. K. Chang, *Bull. Korean Chem. Soc.* **2003**, *24*, 407–408.
- [29] D. J. Mastarone, V. S. R. Harrison, A. L. Eckermann, G. Parigi, C. Luchinat, T. J. Meade, *J. Am. Chem. Soc.* **2011**, *133*, 5329–5337.
- [30] R. S. Ranganathan, E. R. Marinelli, R. Pillai, M. F. Tweedle, *International Pat.*, **1995**, W09527705–A09527701.
- [31] H. Tsukube, Y. Mizutani, S. Shinoda, T. Okazaki, M. Tadokoro, K. Hori, *Inorg. Chem.* **1999**, *38*, 3506–3512.
- [32] Y. Shi, Q. Liu, J. Tang, *Monatsh. Chem.* **2011**, *142*, 907–916.
- [33] G. Haas, V. Prelog, *Helv. Chim. Acta* **1969**, *52*, 1202–1218.
- [34] L. Grisanti, F. Terenziani, C. Sissa, M. Cavazzini, F. Rizzo, S. Orlandi, A. Pannelli, *J. Phys. Chem. B* **2011**, *115*, 11420–11430.

- [35] P. G. Jessop, D. A. Jessop, D. Fu, L. Phan, *Green Chem.* **2012**, *14*, 1245–1259.
- [36] A. Bree, R. Zwarich, *J. Chem. Phys.* **1969**, *51*, 903–912.
- [37] T. Fujii, M. Sano, S. Mishima, H. Hiratsuka, *Bull. Chem. Soc. Jpn.* **1996**, *69*, 1833–1839.
- [38] K. Yoshihara, D. R. Kearns, *J. Chem. Phys.* **1966**, *45*, 1991–1999.
- [39] L. J. Andrews, A. Deroulede, H. Linschitz, *J. Phys. Chem.* **1978**, *82*, 2304–2309.
- [40] K. Binnemans, *Chem. Rev.* **2009**, *109*, 4283–4374.
- [41] R. N. Griffin, *Photochem. Photobiol.* **1968**, *7*, 159–173.
- [42] W. Klöpffer, *Chem. Phys. Lett.* **1971**, *11*, 482–485.
- [43] A. A. Lamola, *J. Chem. Phys.* **1967**, *47*, 4810–4816.
- [44] G. Scharf, J. D. Winefordner, *Talanta* **1986**, *33*, 17–25.
- [45] E. J. J. Groenen, W. N. Koelman, *J. Chem. Soc. Faraday Trans. 2* **1979**, *75*, 69–78.
- [46] P. P. Lima, M. M. Nolasco, F. A. A. Paz, R. A. S. Ferreira, R. L. Longo, O. L. Malta, L. D. Carlos, *Chem. Mater.* **2013**, *25*, 586–598.
- [47] R. A. S. Ferreira, S. S. Nobre, C. M. Granadeiro, H. I. S. Nogueira, L. D. Carlos, O. L. Malta, *J. Lumin.* **2006**, *121*, 561–567.
- [48] M. Bettinelli, A. Speghini, F. Piccinelli, A. N. C. Neto, O. L. Malta, *J. Lumin.* **2011**, *131*, 1026–1028.
- [49] L. Armelao, G. Bottaro, L. Bovo, C. Maccato, M. Pascolini, C. Sada, E. Soini, E. Tondello, *J. Phys. Chem. C* **2009**, *113*, 14429–14434.
- [50] A. Beeby, I. M. Clarkson, R. S. Dickins, S. Faulkner, D. Parker, L. Royle, A. S. de Sousa, J. A. Gareth Williams, M. Woods, *J. Chem. Soc. Perkin Trans. 2* **1999**, 493–504.
- [51] W. D. Horrocks, D. R. Sudnick, *Acc. Chem. Res.* **1981**, *14*, 384–392.
- [52] S. T. Frey, W. D. Horrocks, Jr, *Inorg. Chim. Acta* **1995**, *229*, 383–390.
- [53] R. M. Supkowski, W. D. Horrocks, Jr, *Inorg. Chim. Acta* **2002**, *340*, 44–48.
- [54] Y. Ma, Y. Wang, *Coord. Chem. Rev.* **2010**, *254*, 972–990.
- [55] P. Nockemann, E. Beurer, K. Driesen, R. Van Deun, K. Van Hecke, L. Van Meervelt, K. Binnemans, *Chem. Commun.* **2005**, 4354–4356.
- [56] J. Kai, M. C. F. C. Felinto, L. A. O. Nunes, O. L. Malta, H. F. Brito, *J. Mater. Chem.* **2011**, *21*, 3796–3802.
- [57] P. P. Lima, R. A. S. Ferreira, R. O. Freire, F. A. Almeida Paz, L. Fu, S. Alves, L. D. Carlos, O. L. Malta, *ChemPhysChem* **2006**, *7*, 735–746.
- [58] X. Y. Chen, M. P. Jensen, G. K. Liu, *J. Phys. Chem. B* **2005**, *109*, 13991–13999.
- [59] J. W. Walton, R. Carr, N. H. Evans, A. M. Funk, A. M. Kenwright, D. Parker, D. S. Yufit, M. Botta, S. De Pinto, K.-L. Wong, *Inorg. Chem.* **2012**, *51*, 8042–8056.
- [60] A. M. Brouwer, *Pure Appl. Chem.* **2011**, *83*, 2213–2228.

Received: December 24, 2013

Revised: February 7, 2014

Published online on March 25, 2014